Materials Research Proceedings **27** (2023) 150-157 https://doi.org/10.21741/9781644902455-19

Construct the seismic response analysis model of an existing nuclear facility using 4SID

Rino Kato[1,a,*], Takenori Hida[1,b], Hideaki Tsutsumi[2,c], and Tsuyoshi Takada[3,d]

[1]Graduate School of Sci. and Eng., Ibaraki Univ., Hitachi-shi, Ibaraki, Japan

[2]Total Support System Corporation, Naka-Gun, Ibaraki, Japan

[3]Japan Atomic Energy Agency, Naka-Gun, Ibaraki, Japan

[a]22nm809r@vc.ibaraki.ac.jp, [b]takenori.hida.mn75@vc.ibaraki.ac.jp, [c]tsutsumi.hideaki@jaea.go.jp, [d]takada.tsuyoshi@jaea.go.jp

Keywords: Nuclear Facility, Strong Motion Records, Seismic Response Analysis, Sway–Rocking Model, Hierarchical Clustering, Subspace State Space System Identification

Abstract The seismic response analysis model of a nuclear facility can be used to evaluate the integrity of the structure as well as the safety of humans and machines within in the event of an earthquake. This study accordingly proposed a methodology for constructing the seismic response analysis model of a nuclear facility based on observed strong motion records. First, to evaluate the seismic response characteristics of an example nuclear facility in Japan, the subspace state-space system identification [1] technique was applied to strong motion records from the 2011 off the Pacific coast of Tohoku Earthquake. The identified natural modes were then clustered using the hierarchical clustering technique. Second, a seismic response analysis model of the example facility was constructed for each cluster based on the sway–rocking model. The stiffness and damping factors for each model were calculated from the mean values of the corresponding mode characteristics. Third, the constructed models were employed for seismic response analysis using the strong motion record observed during the main shock of the 2011 Tohoku earthquake as input, and the root mean square errors between the response records and analytical results were evaluated to select the most accurate model. Finally, the selected model was validated by performing a seismic response analysis using the strong motion records from an aftershock of the 2011 Tohoku earthquake. The analytical responses showed good agreement with the records, indicating that the proposed method represents a valid approach for constructing seismic response analysis models of nuclear facilities.

Introduction

A seismic analysis model is useful for assessing not only the structural integrity of a building during an earthquake but also the safety of humans and machines inside. Many studies have been conducted to investigate methodologies for evaluating the seismic response characteristics of a building using subspace state-space system identification (4SID) [2]. However, few studies have undertaken seismic response analyses of nuclear facilities based on strong motion records using 4SID. This paper therefore proposes a methodology for constructing a seismic response model based on the strong motion records observed at an existing nuclear facility.

To evaluate the vibration characteristics of the example nuclear facility, the 4SID technique was applied to the strong motion response records observed at the facility during the 2011 off the Pacific coast of Tohoku Earthquake. The characteristics of the natural modes were then clustered by a hierarchical clustering technique. Next, a seismic response analysis model of the facility was constructed using the sway–rocking (SR) model to consider the soil–structure interaction through the combined action of a rocking spring and sway spring installed between the substructure and the ground. Finally, the proposed method was verified by inputting the strong motion record from

an aftershock of the 2011 Tohoku earthquake into the constructed model and comparing its responses with the corresponding response records.

Methodology of Subspace State-space System Identification

In this study, the ordinary multivariable output-error state space [1], which is a 4SID algorithm, was used to identify the seismic response characteristics of an example nuclear facility. The discrete-time linear time-invariant system is expressed by the state-space expression as follows:

$$\begin{cases} \mathbf{x}(t+1) = \mathbf{A}\mathbf{x}(t) + \mathbf{B}\mathbf{u}(t) \\ \mathbf{y}(t) = \mathbf{C}\mathbf{x}(t) + \mathbf{D}\mathbf{u}(t) \end{cases} \tag{1}$$

where $\mathbf{x}(t)$ is the state vector, $\mathbf{u}(t)$ is the input vector, $\mathbf{y}(t)$ is the output vector, and **A**, **B**, **C,** and **D** are constant matrices.

For *r*-input and *m*-output systems, the block Hankel matrix, which consists of input and output data **U** and **Y**, respectively, can be constructed as follows:

$$\mathbf{U} = \begin{bmatrix} \mathbf{u}_1 & \mathbf{u}_2 & \cdots & \mathbf{u}_{N-\nu+1} \\ \mathbf{u}_2 & \mathbf{u}_3 & \cdots & \mathbf{u}_{N-\nu+2} \\ \vdots & \vdots & \ddots & \vdots \\ \mathbf{u}_\nu & \mathbf{u}_{\nu+1} & \cdots & \mathbf{u}_N \end{bmatrix}, \qquad \mathbf{Y} = \begin{bmatrix} \mathbf{y}_1 & \mathbf{y}_2 & \cdots & \mathbf{y}_{N-\nu+1} \\ \mathbf{y}_2 & \mathbf{y}_3 & \cdots & \mathbf{y}_{N-\nu+2} \\ \vdots & \vdots & \ddots & \vdots \\ \mathbf{y}_\nu & \mathbf{y}_{\nu+1} & \cdots & \mathbf{y}_N \end{bmatrix} \tag{2}$$

where *N* and *v* denote the number of data points and the number of block rows, respectively.

Then, matrix **Ξ** is calculated using the following equation:

$$\mathbf{\Xi} = \mathbf{Y}\mathbf{\Pi}_\mathbf{U}^\perp \tag{3}$$

where $\mathbf{\Pi}_\mathbf{U}^\perp$ is the geometric operator that projects the row space of matrix **Y** onto the orthogonal complement of the row space of matrix **U**. This is represented by the following equation:

$$\mathbf{\Pi}_\mathbf{U}^\perp = \mathbf{I} - \mathbf{U}^T(\mathbf{U}\mathbf{U}^T)^{-1}\mathbf{U} \tag{4}$$

where **I** is an identity matrix and *T* denotes transposition.

The singular value decomposition of **Ξ** is performed according to the following equation:

$$\mathbf{\Xi}_N = \begin{bmatrix} \mathbf{U}_1 & \mathbf{U}_2 \end{bmatrix} \begin{bmatrix} \mathbf{\Sigma}_1 & \\ & \mathbf{\Sigma}_2 \end{bmatrix} \begin{bmatrix} \mathbf{V}_1 \\ \mathbf{V}_2 \end{bmatrix} \tag{5}$$

where *n* denotes the system order, $\mathbf{\Sigma}_1$ and $\mathbf{\Sigma}_2$ comprise the diagonal matrix consisting of the singular value of **Ξ**, and $\mathbf{U}_1$, $\mathbf{U}_2$, $\mathbf{V}_1$, and $\mathbf{V}_2$ denote the singular matrices.

The extended observability matrix $\mathbf{\Theta}$ is calculated using:

$$\mathbf{\Theta}_\nu = \mathbf{U}_1\mathbf{\Sigma}_1^{1/2} = \begin{bmatrix} \mathbf{C} \\ \mathbf{C}\mathbf{A} \\ \vdots \\ \mathbf{C}\mathbf{A}^{r-1} \end{bmatrix} \tag{6}$$

Matrix **C** can be identified from the upper block matrix of $\mathbf{\Theta}_\nu$; matrix **A** can be identified as follows:

$$\mathbf{A} = \underline{\mathbf{\Theta}}_\nu^\dagger \overline{\mathbf{\Theta}}_\nu = \begin{bmatrix} \mathbf{C} \\ \mathbf{C}\mathbf{A} \\ \vdots \\ \mathbf{C}\mathbf{A}^{r-2} \end{bmatrix}^\dagger \begin{bmatrix} \mathbf{C}\mathbf{A} \\ \mathbf{C}\mathbf{A} \\ \vdots \\ \mathbf{C}\mathbf{A}^{r-1} \end{bmatrix} \tag{7}$$

where † denotes the Moore–Penrose pseudo inverse matrix [5][6].

The natural circular frequency ω_j, damping ratio h_j, and eigenmode vector **Φ** of the *j*-th eigenmode are calculated by the following equations:

$$\omega_j = \frac{\left|\ln \lambda_j\right|}{\Delta t}, \qquad h_j = -\frac{\ln\left|\lambda_j\right|}{\left|\ln \lambda_j\right|}, \qquad \mathbf{\Phi} = \mathbf{C}\phi_j \tag{8}$$

where λ_j, Δt, and φ_j denote the j-th eigenvalue of matrix **A**, the sampling period, and the eigenvector of matrix **A,** respectively.

Seismic Analysis Model

The section of the example nuclear facility is illustrated in Figure 1, and its corresponding SR model is shown in Figure 2. In this paper, the nuclear facility was modelized by SR model.

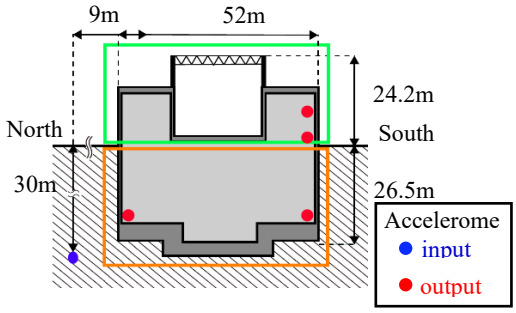

Fig. 1 Section view of the subject nuclear facility building

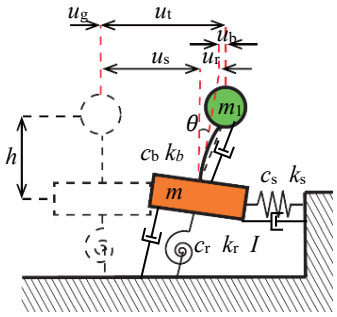

Fig. 2 SR model of the subject building

The model shown in Figure 2 consists of two masses: m_1 corresponding to the superstructure and m_2 corresponding to the substructure. Their combined equation of motion is given by:

$$\left\{\left(\frac{\ln\lambda'}{\Delta t}\right)^2\begin{bmatrix} m_1 & & \\ & m_2 & \\ & & J \end{bmatrix} + \left(\frac{\ln\lambda'}{\Delta t}\right)\begin{bmatrix} c_b & -c_b & c_b h \\ -c_b & c_b + c_s & c_b h \\ -c_b h & c_b h & c_b h^2 + c_r \end{bmatrix} + \begin{bmatrix} k_b & -k_b & k_b h \\ -k_b & k_b + k_s & k_b h \\ -k_b h & k_b h & k_b h^2 + k_r \end{bmatrix}\right\}\begin{Bmatrix} U_t \\ U_s \\ \Theta \end{Bmatrix} = \mathbf{O} \tag{9}$$

where J is the rotational inertia of the substructure; k_b, k_s, and k_r are the rigidities of the superstructure, sway spring, and rotational spring, respectively; c_b, c_s, and c_r are the damping coefficients of the superstructure, sway spring, and rotational spring, respectively; λ' is the identified complex eigenvalue of matrix A; h is the height of the superstructure; Δt is the sampling period of the strong motion record; U_t and U_s are the horizontal mode amplitudes of the superstructure and substructure, respectively; and Θ denotes the angular amplitude of the substructure.

The rigidities and damping coefficients of the system can be calculated using the following equations:

$$\begin{Bmatrix} c_b \\ k_b \\ c_s \\ k_s \\ c_r \\ k_r \end{Bmatrix} = \begin{bmatrix} \mathrm{Re}(X\Lambda) & \mathrm{Re}(X) & & & & \\ \mathrm{Re}(X\Lambda) & \mathrm{Im}(X) & & & & \\ -\mathrm{Re}(X\Lambda) & -\mathrm{Re}(X) & -\mathrm{Re}(U_s\Lambda) & \mathrm{Re}(U_s) & & \\ -\mathrm{Im}(X\Lambda) & -\mathrm{Im}(X) & -\mathrm{Im}(U_s\Lambda) & \mathrm{Im}(U_s) & & \\ -\mathrm{Re}(X\Lambda)h & -\mathrm{Re}(X)h & & & -\mathrm{Re}(\Theta\Lambda) & \mathrm{Re}(\Theta) \\ -\mathrm{Im}(X\Lambda)h & -\mathrm{Im}(X)h & & & -\mathrm{Im}(\Theta\Lambda) & \mathrm{Im}(\Theta) \end{bmatrix}^{-1} \begin{Bmatrix} \mathrm{Re}(-\Lambda^2 U_t)m_1 \\ \mathrm{Im}(-\Lambda^2 U_t)m_1 \\ \mathrm{Re}(-\Lambda^2 U_s)m_2 \\ \mathrm{Im}(-\Lambda^2 U_s)m_2 \\ \mathrm{Re}(-\Lambda^2\Theta)J \\ \mathrm{Im}(-\Lambda^2\Theta)J \end{Bmatrix} \tag{10}$$

$$X = U_t - U_s - h\Theta \tag{11}$$

$$\Lambda = \ln\lambda'/\Delta t \tag{12}$$

where X is superstructure's relative displacement.

Materials Research Proceedings **27** (2023) 150-157 https://doi.org/10.21741/9781644902455-19

System Identification

The strong motion records depicting the north–south component observed at the example nuclear facility during the 2011 off the Pacific coast of Tohoku Earthquake are shown in Figure 3. Note that the acceleration amplitude of the superstructure was larger than that of the substructure and input motion.

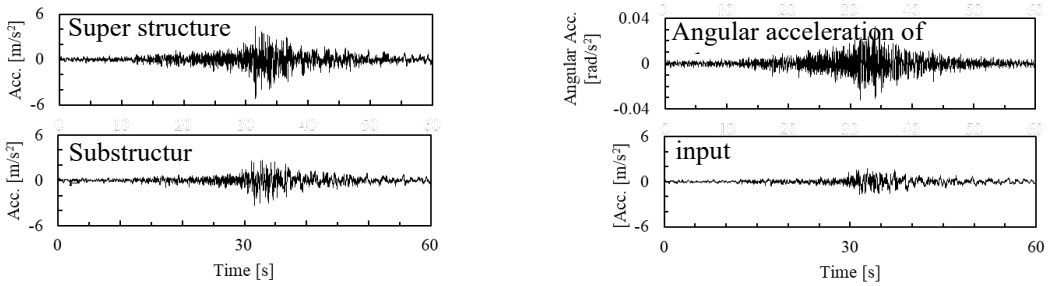

Fig. 3 Acceleration time history waveforms

Figure 4 shows the transfer function identified by 4SID with system orders of 6 and 14. When the system order was set to 6 and 14, the natural frequencies were identified including approximately 3 Hz, 6.8 Hz, and 9.2 Hz.

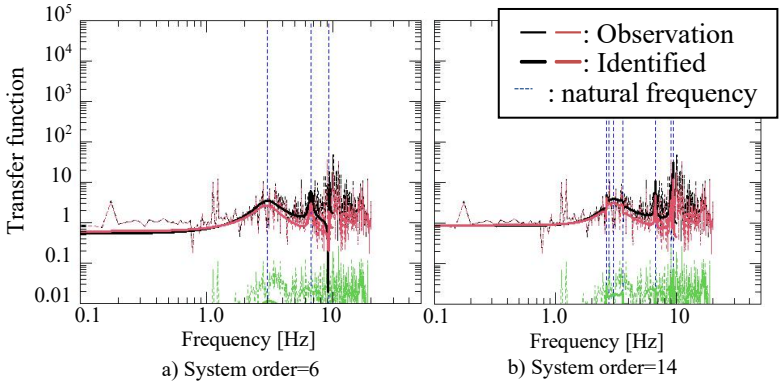

Fig. 4 Transfer functions for a system order of (a) 6 and (b) 14

Figure 5 shows a stabilization diagram representing the relationship between the natural frequencies and system orders. Although the eigenmodes were slightly scattered, the natural frequencies of the first, second, and third modes can indeed be identified at approximately 3 Hz, 6.8 Hz, and 9.2 Hz, respectively.

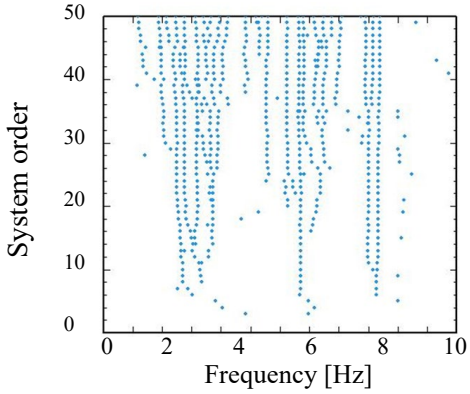

Fig. 5 Stabilization diagram

Materials Research Proceedings **27** (2023) 150-157 https://doi.org/10.21741/9781644902455-19

To evaluate the valid eigenmode, a hierarchical clustering technique was applied to the system identification results. The modal assurance criterion (MAC) was used as the cluster distance to evaluate the similarity between any two eigenmodes as follows:

$$MAC_{ij} = \frac{\left|\varphi_i^T \varphi_j^*\right|^2}{\left\{\varphi_i^T \varphi_i^*\right\}\left\{\varphi_j^T \varphi_j^*\right\}} \qquad (0 \le MAC_{ij} \le 1) \tag{12}$$

where φ_i denotes the i-th mode vector and * denotes conjugation. Ranging from 0 to 1, the larger the MAC value, the more similar the two compared modes. The distance between the two compared eigenmodes was calculated using [4]:

$$d_{ij} = \left|\frac{f_i - f_j}{f_j}\right| + (1 - MAC_{ij}) \tag{13}$$

Figure 6 shows the relationship between the cluster number ratio and cluster distance. In this study, clustering was terminated when the cluster number ratio reached 10%.

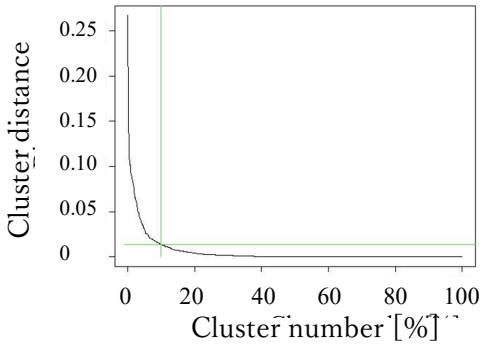

Fig. 6 Relationship between cluster number and distance

Figure 7 shows the relationship between the identified natural frequencies and damping ratios. Markers with the same color and shape indicate results belonging to the same cluster. The red marker was each center of cluster. The natural frequency of both the black and yellow clusters was determined to be approximately 3 Hz, suggesting that they correspond to the first mode. The natural frequency of the blue cluster was approximately 6.8 Hz and that of the green cluster was approximately 9.2 Hz, suggesting that these clusters correspond to the second and third modes, respectively.

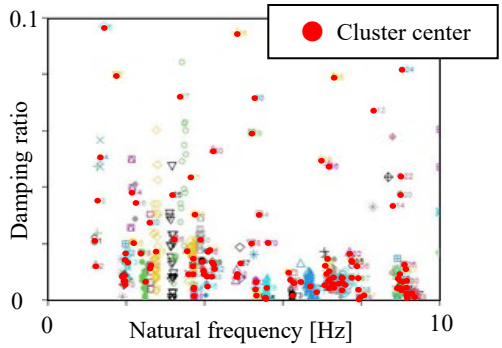

Fig. 7 Relationships between natural frequencies and

Construction and Validation of the Seismic Response Analysis Model

This section describes the methodology used to construct the SR models of the example nuclear facility based on the system identification results. First, the cluster results indicating a damping ratio greater than 0.06 were excluded. Then, based on Equation (7) as well as the masses and rotational inertias given in Table 1, the stiffness and damping coefficients were calculated from the averaged eigenvalue and eigenmode vector for each cluster to construct a series of models.

Seismic response analyses using the Newmark-β method (β = 1/4, γ = 1/2) were performed on all constructed models by applying the strong motion record from the main shock of the 2011 off the Pacific coast of Tohoku Earthquake as input. Then, the root mean square errors (RMSEs) between the acceleration time histories provided in the analytical results and the corresponding strong motion response records were calculated, and the model with the lowest RMSE was selected as the best model. The natural frequency and damping ratio obtained in this study for the best model were 2.51 Hz and 0.069, respectively.

Table 1 Hyperparameters of system identification, mass, and rotational inertia

system order	2~50
number of lines of block matrix	60
m_1	1.7×10^7 [kg]
m_2	5.8×10^7 [kg]
I	1.6×10^2 [kg·m^2]

The acceleration and velocity time-history waveforms of the best model under the strong motion records input are compared with the observed response records in Figure 8. The amplitudes and phases of the horizontal accelerations of the model superstructure and substructure showed excellent agreement with the observed response accelerations, whereas the modeled angular acceleration of the substructure departed somewhat from the observed response.

To validate the derived analysis model, the seismic responses were calculated using the time-history waveform observed during an aftershock of the 2011 off the Pacific coast of Tohoku Earthquake as input. The results are provided in Figure 9, which shows that although the angular acceleration and velocity of the model substructure were poorly reproduced, the horizontal accelerations and velocities of the model superstructure and substructure correspond well with the response records, confirming the validity of the model.

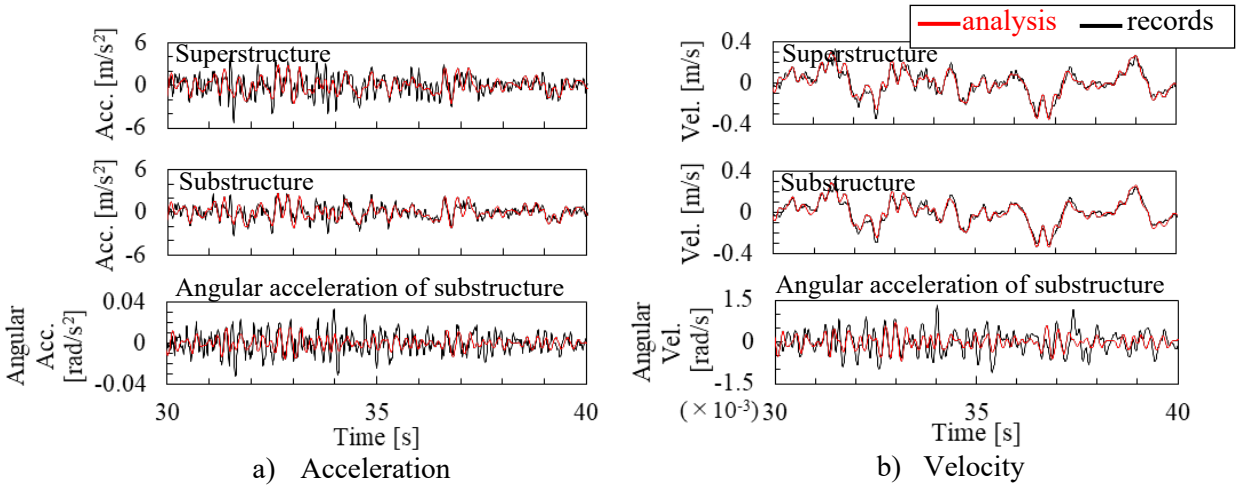

Fig. 8 Comparison of model time-history waves with records of main shock acceleration and velocity

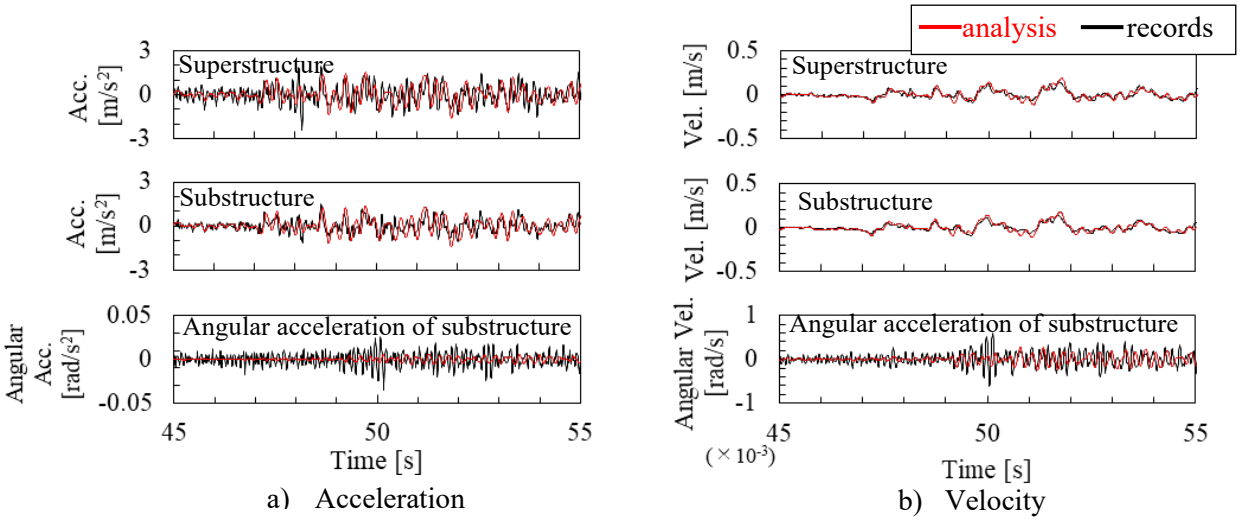

Fig. 9 Comparison of model time-history waves with records of aftershock acceleration and velocity

Conclusion

In this study, a methodology for constructing the seismic response analysis model of a nuclear facility was demonstrated using the results of system identification using 4SID. This study accomplished the following:

1) A method was derived to determine the stiffness and damping coefficients of the SR model using the average of the eigenvalues and eigenmode vectors from the system identification results obtained using 4SID.
2) The system identification results were clustered, the stiffness and damping coefficients were calculated for each cluster, and seismic response models were constructed accordingly. The most valid analytical model was identified by conducting a seismic response analysis subjecting each model to the same input motion and then selecting the model with the smallest RMSE value relative to the corresponding strong motion response records.

3) The results obtained when inputting a strong motion record that was not used for system identification into the selected response analysis model agreed well with the corresponding response records, confirming the validity of the proposed method.

Acknowledgement
This study was supported by the Japan Atomic Energy Agency (JAEA), who also provided the strong motion records used in this study.

References

[1] M. Verhaegen and P. Dewilde: Subspace model identification Part 1. The output-error state-space model identification class of algorithms, *International Journal of Control*, Vol. **56**, No. 5, pp. 1187–1210, 1992. https://doi.org/10.1080/00207179208934363

[2] T. Tojo and S. Nakak: Identification of sway rocking spring and pile damage detection using subspace method, Vol. **87**, No. 791, pp. 60–71, 2022. https://doi.org/10.3130/aijs.87.60

[3] R. J. Allemang: The Modal Assurance Criterion (MAC), Structural Dynamics Research Laboratory Mechanical, Industrial and Nuclear Engineering OH 45221-0072 USA

[4] R. J. Allemang and D. L. Brown: Correlation Coefficient for Modal Vector Analysis, *Proceedings of the International Modal Analysis Conference*, pp. 110–116, 1982

[5] E. H. Moore: On the reciprocal of the general algebraic matrix, *Bulletin of the American Mathematical Society*, Vol. **26**, pp. 394–395, 1920. https://doi.org/10.1090/S0002-9904-1920-03332-X

[6] R. Penrose: A generalized inverse for matrices, *Proceedings of the Cambridge Philosophical Society*, Vol. **51**, No. 3, pp. 406–413, 1955. https://doi.org/10.1017/S0305004100030401